Geochemistry Geophysics Geosystems G3

Published by AGU and the Geochemical Society

Article
Volume 13, Number 1
23 March 2012
Q03019, doi:10.1029/2011GC004015
ISSN: 1525-2027

First paleomagnetic results of mid- to late Holocene sediments from Lake Issyk-Kul (Kyrgyzstan): Implications for paleosecular variation in central Asia

Miriam Gómez-Paccard
Institute of Earth Sciences Jaume Almera, CSIC, Lluís Solé i Sabarís s/n, E-08028 Barcelona, Spain (mgomezpaccard@ictja.csic.es)

Juan C. Larrasoaña
Unidad de Zaragoza, Instituto Geológico y Minero de España, Manuel Lasala 44, 9B, E-50006 Zaragoza, Spain (jc.larra@igme.es)

Santiago Giralt
Institute of Earth Sciences Jaume Almera, CSIC, Lluís Solé i Sabarís s/n, E-08028 Barcelona, Spain (sgiralt@ictja.csic.es)

Andrew P. Roberts
Research School of Earth Sciences, Australian National University, Canberra, ACT 0200, Australia (andrew.roberts@anu.edu.au)

[1] We present new paleomagnetic and rock magnetic data from mid and late Holocene sediments recovered in two gravity cores (C087 and C142a) from Lake Issyk-Kul (central Asia), for which independent radiocarbon-based age models are available. Our results indicate that sediments from core C087 are characterized by fine (pseudo single domain) magnetite grains and are reliable recorders of Holocene geomagnetic paleosecular variation (PSV) in central Asia, which is a region with poor data coverage. Similarity is found between the core C087 PSV record, which spans the last 5700 years, and the Lake Baikal PSV record, which is the only published Holocene central Asian PSV record of comparable length with an independent radiocarbon-based chronology. Our new results represent a step forward in constructing a reference PSV curve for central Asia that can be used to date sedimentary sequences. These results can also be used to improve the reliability and accuracy of global geomagnetic field models. We have not been able to disentangle past environmental changes in the Lake Issyk-Kul region based on rock magnetic properties, probably because the magnetite and hematite in the studied sediments have a mixed (fluvial and eolian) terrigenous origin.

Components: 8600 words, 7 figures, 1 table.

Keywords: Holocene; central Asia; lacustrine sediments; paleomagnetism; rock magnetism; secular variation.

Index Terms: 1522 Geomagnetism and Paleomagnetism: Paleomagnetic secular variation; 1532 Geomagnetism and Paleomagnetism: Reference fields: regional, global; 1540 Geomagnetism and Paleomagnetism: Rock and mineral magnetism.

Received 19 December 2011; **Revised** 15 February 2012; **Accepted** 20 February 2012; **Published** 23 March 2012.

Gómez-Paccard, M., J. C. Larrasoaña, S. Giralt, and A. P. Roberts (2012), First paleomagnetic results of mid- to late Holocene sediments from Lake Issyk-Kul (Kyrgyzstan): Implications for paleosecular variation in central Asia, *Geochem. Geophys. Geosyst.*, *13*, Q03019, doi:10.1029/2011GC004015.

1. Introduction

[2] Documentation of geomagnetic field variations provides important information on the operation of the geodynamo and on links between solar activity and Earth's climate via improved interpretations of cosmogenic isotopes [*Muscheler et al.*, 2005]. Geomagnetic field changes can also have important applications in geochronologic studies of Quaternary sediments [e.g., *Snowball et al.*, 2007; *Lisé-Pronovost et al.*, 2009; *Barletta et al.*, 2010] and for testing the controversial hypothesized links between Earth's magnetic field and climate [e.g., *Wollin et al.*, 1978; *Gallet et al.*, 2005; *Snowball and Muscheler*, 2007; *Courtillot et al.*, 2007; *Bard and Delaygue*, 2008; *Gómez-Paccard et al.*, 2008]. Beyond instrumental records available for the last 400 years, past geomagnetic field variations are best obtained from fired archeological materials and volcanic rocks. The magnetic signals recorded by these materials are thermoremanent magnetizations [*Néel*, 1955], which provide accurate paleomagnetic directions and enable determination of absolute paleointensities. Well-dated sedimentary records can also give reliable information on changes in the direction and relative intensity of the geomagnetic field [e.g., *Stockhausen*, 1998; *Ali et al.*, 1999; *Frank et al.*, 2002; *Vigliotti*, 2006; *Irurzun et al.*, 2006, 2008; *Snowball et al.*, 2007]. Rapidly deposited sediments are often targeted for geomagnetic field studies due to the possibility of obtaining information on shorter period variations than can be obtained from archeomagnetic and volcanic data throughout the Holocene.

[3] Archeomagnetic, volcanic and sedimentary data can be used to construct regional curves of both the direction and intensity of the geomagnetic field [e.g., *Gómez-Paccard et al.*, 2006, 2008; *Snowball et al.*, 2007] or to compute regional or global geomagnetic field models [e.g., *Pavón-Carrasco et al.*, 2009; *Korte and Constable*, 2005; *Korte et al.*, 2009] that can help to describe the temporal and spatial behavior of the geomagnetic field on centennial timescales. The accuracy and reliability of such curves and models relies on the quality, quantity and the spatial and temporal distribution of the paleomagnetic data used for their construction. A crucial issue for improving the reliability of geomagnetic field models is the fidelity of the data used for their construction. Thus, chronological uncertainties associated with the input data affect the temporal resolution of the models and strongly influence the structure of the modeled magnetic field variations [*Korte and Constable*, 2005]. One of the regions in the world with strikingly poor data coverage is central Asia, where only three sedimentary paleosecular variation (PSV) records are available for the last six millennia from a region that covers more than 24×10^6 km^2 (about 5% of the Earth's surface) and extends from about 6 to 43.5°N and 54 to 107°E (Figure 1a). The Lake Aslikul record spans from 2450 yr BC to 1900 yr AD [*Nurgaliev et al.*, 1996] with high temporal resolution (~10 yr). The Aral Sea PSV record also has high resolution (~25 yr), but spans (only) 525 to 1675 yr [*Nourgaliev et al.*, 2003]. The Lake Baikal record [*Peck et al.*, 1996] covers from 1575 yr AD to beyond the Holocene with much lower resolution (~150 yr). Variable geomagnetic field changes are expected over this vast region. Therefore, new PSV data from this region are important for constructing geomagnetic field models.

[4] We present a new paleomagnetic and rock-magnetic study of mid to late Holocene sediments from Lake Issyk-Kul (Figure 1), which were recovered in two gravity cores (C142a and C087) for which independent radiocarbon-based age models are available [*Larrasoaña et al.*, 2011]. Our results contribute to improving PSV data coverage in a virtually unexplored region and can be used to test and improve geomagnetic field models. Rock magnetic data are used to assess the reliability of the PSV record obtained and to discuss the significance of environmental variations in the studied sediments for the last six millennia.

2. Geological Setting and Methods

[5] Lake Issyk-Kul (182 km long, 60 km wide, 668 m deep, 1607 m a.s.l.) is a large, endorheic and slightly saline lake (about 6 g/l of total dissolved solids) that is located in one of the largest Neogene intermontane basins of the Tien Shan range (Figure 1a). The lake is located between the Kungey (to the north) and Terzkey (to the south) ranges (Figure 1b), which reach altitudes of up to nearly 6000 m a.s.l. and are mainly composed of Pre-Cambrian and Paleozoic crystalline rocks [*Torizin et al.*, 2009]. The lake has a relatively small catchment (250 km long and 100 km wide) compared with the size of the lake [*Zabirov and Korotaev*, 1978]. There are about 100 streams and rivers that feed the lake. The two largest rivers (Jergueland and Tyup) are located to the east of the lake. They are predominantly fed by meltwater from glaciers and snow from the Terzkey Ranges. One of the most noticeable features of the lake is the annual lake level oscillation of about 40 cm

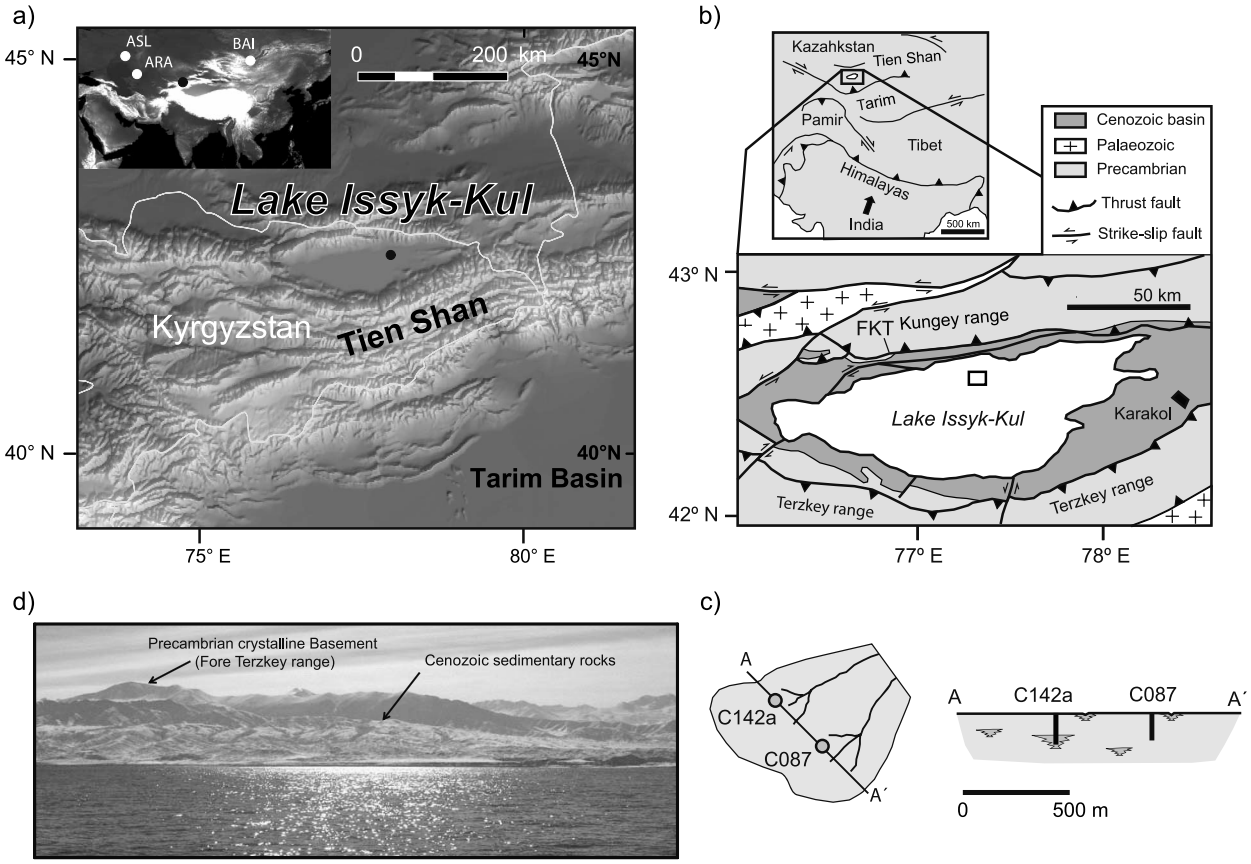

Figure 1. (a) Location of Lake Issyk-Kul, and of other lacustrine records mentioned (ASL: Lake Aslikul; BAI: Lake Baikal; ARA: Aral Sea). (b) Geological sketch map of the Lake Issyk-Kul basin and surrounding mountain ranges in the context of India-Asia collision (FKT: Fore Kungey Thrust). The black dot (box) in Figure 1a (Figure 1b) denotes the location of the studied cores. (c) Sketch of the location of the studied cores (with schematic geologic cross-section) within a lobe of the deltaic system that drains the northern shore of Lake Issyk-Kul [after *Larrasoaña et al.*, 2011]. (d) Southwestern shore of Lake Issyk-Kul viewed from the center of the lake.

associated with the main precipitation peak and ice and snow melting (spring and summer) and ice and snow accumulation (autumn and winter) in the ice caps of the surrounding mountains. The sedimentary infill of Lake Issyk-Kul consists of a mixture of lacustrine carbonates and riverine and eolian terrigenous sediments that record Miocene through Holocene deposition [*De Batist et al.*, 2002; *Giralt et al.*, 2004]. In August 2000, two azimuthally unoriented continuous gravity cores, C142a (42°34′31.2″N, 77°20′03.0″E) and C087 (42°34′5.22″N, 77°20′10.44″E), were retrieved on board the R/V *Moltur* from the central northern shore of the lake at water depths of 150 and 312 m, respectively (Figure 1). Core C142a comprises a 150-cm-thick sequence of Late Holocene clays, silts and sandy silts that accumulated in a distal lobe of the deltaic system that drains into the lake along a NE-SW direction [*De Batist et al.*, 2002; *Larrasoaña et al.*, 2011] (Figures 1b and 1c). Core C087 comprises 132 cm of clays and silty clays that are equivalent to those in the uppermost 94 cm of core C142a. The lack of coarser-grained sediments at the base of core C087 might be explained by the discontinuous nature of deltaic tributary systems (Figure 1c).

[6] Paleomagnetic samples were obtained by pushing plastic boxes (2 × 2 × 2 cm) continuously into the working half of cores C142a and C087. Paleomagnetic analyses were performed at the paleomagnetic laboratory of the Institute of Earth Sciences Jaume Almera (UB-CSIC) in Barcelona. They involved measurement of the low-field magnetic susceptibility (χ) and progressive alternating field (AF) demagnetization of the natural remanent magnetization (NRM) of all samples. Stepwise AF demagnetization experiments were conducted

at 5–10 mT steps and up to a maximum field of 80–100 mT. Stable characteristic remanent magnetization (ChRM) directions were identified through visual inspection of orthogonal demagnetization plots [*Zijderveld*, 1967], and were calculated by fitting linear trends in the demagnetization plots using principal component analysis [*Kirschvink*, 1980]. Additional rock magnetic properties that were measured include the anhysteretic remanent magnetization (ARM) and two isothermal remanent magnetizations that were imparted at 0.1 T ($IRM_{0.1\ T}$) and 1.2 T ($IRM_{1.2\ T}$). χ was measured with a Kappabridge KLY-2 (Geofyzica Brno) susceptibility bridge using a field of 0.1 mT at a frequency of 470 Hz. AF demagnetization and ARM experiments were conducted using a D-Tech 2000 (ASC Scientific) AF demagnetizer. The ARM was applied along the Z axis of the samples with a dc bias field of 0.05 mT parallel to a peak AF of 100 mT. $IRM_{0.1\ T}$ and $IRM_{1.2\ T}$ were imparted using an IM10–30 (ASC Scientific) pulse magnetizer. Magnetizations were measured using a SRM755R (2G Enterprises) three-axis cryogenic superconducting rock magnetometer.

[7] We used different magnetic properties and interparametric ratios to determine down-core variations in the type, concentration, and grain size of magnetic minerals. Magnetic susceptibility (χ) has been used as a first-order indicator of the concentration of magnetic (*sensu lato*) minerals. We have calculated the forward S-ratio (or S′-ratio [see *Kruiver and Passier*, 2001]), which is defined as $IRM_{0.1\ T}/IRM_{1.2\ T}$ and is equivalent to the S-ratio of *Bloemendal et al.* [1992]. This S-ratio has been used to indicate the relative concentration of low versus high coercivity minerals. ARM has been used as a proxy for the concentration of low coercivity minerals [e.g., *Evans and Heller*, 2003]. $IRM_{1.2\ T} - IRM_{0.1\ T}$, which is equivalent to the "hard" IRM of *Bloemendal et al.* [1992] (hereafter referred to as HIRM), has been used as a proxy for the concentration of high coercivity minerals. Finally, the $IRM_{1.2\ T}/\chi$ ratio has been used to make inferences about the dominant magnetic minerals in a sedimentary sequence [e.g., *Peters and Dekkers*, 2003] and about relative variations in magnetic mineral grain size, provided that a single magnetic mineral is dominant [*Thompson and Oldfield*, 1986; *Verosub and Roberts*, 1995; *Evans and Heller*, 2003]. Hysteresis measurements for samples from different depths within each core were made using a Princeton Measurements Corporation vibrating sample magnetometer at the Kochi Core Center (Japan) and at the Institute for Rock Magnetism (Minneapolis, USA) to establish the domain state of the magnetic minerals [*Day et al.*, 1977; *Dunlop*, 2002].

[8] Auxiliary geochemical data include the iron (Fe) and total organic carbon (TOC) contents for core C142a. The Fe content was measured every 0.3 mm with an ITRAX XRF core scanner at the University of Vigo. A mean value every 2 cm was calculated using a running average. TOC was measured every centimeter using a UIC model 5011 CO_2 Coulometer at the Technical Services of the University of Barcelona. All magnetic and geochemical properties are reported in terms of the dry weight of the samples.

3. Stratigraphy, Sedimentology, and Age Models for the Studied Sediments

[9] Cores C142a and C087 consist of laminated clays, silts and silty-clays that are arranged into two main lithologic units (Figure 2). The upper unit includes the uppermost 18 cm and 13 cm of cores C142a and C087, respectively, and is mainly composed of dark and massive silty-clays. The lower unit extends to the bottom of both cores and is made up of alternating millimeter- to centimeter-scale laminae that consist of light and dark gray clays. Sediments in core C142a have a slightly coarser texture in the lowermost 56 cm. Light-colored laminae are mainly composed of a fine mixture of massive micritic carbonate with other terrigenous minerals such as quartz and phyllosilicates and frequent fragments and whole shells of ostracods and diatoms. Dark-colored lamina consist of massive micritic carbonate with large fragments of partially pyritized plant remains and charcoal, as well as patchy black sulfide-and/or manganese-rich accumulations. Millimeter-scale alternations of these laminae appear to be associated with annual water level oscillations, which are driven by the spring melting of surrounding mountain ice caps and accumulation of ice and snow in autumn. On the other hand, centimeter-scale alternations of laminae seem to be related to early diagenetic conditions linked to degradation of organic matter (see *Giralt et al.* [2002] for further details).

[10] Based on available sedimentologic data, the studied sediments can be interpreted as distal prodeltaic sediments that accumulated on the lake shelf. These sediments are mainly characterized by endogenic carbonates and variable contributions from both riverine (from the Jergueland and Tyup rivers) and eolian (from the Taklamakan Desert in

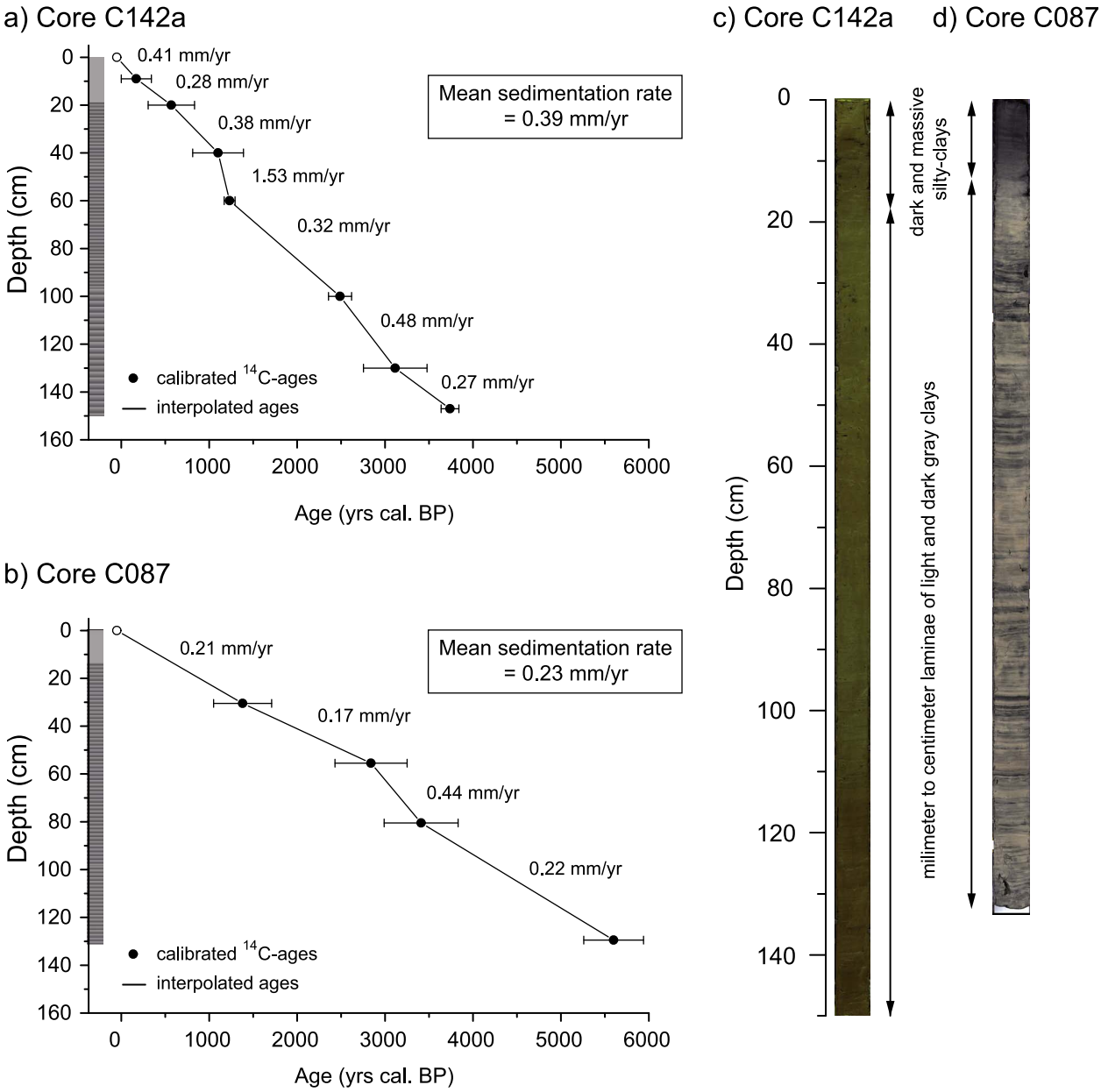

Figure 2. Age models for cores (a) C142a and (b) C087 (see *Larrasoaña et al.* [2011] for details). The age models are based on AMS radiocarbon datings of pollen-enriched samples (black dots). Lithostratigraphic columns of the studied Holocene sediments from Lake Issyk-Kul, cores (c) C142a and (d) C087. The sedimentation rates derived from the age models are indicated in Figures 2a and 2b.

the Tarim basin and other sources) terrigenous material [*De Batist et al.*, 2002; *Giralt et al.*, 2004].

[11] Establishment of an independent chronological framework is crucial to obtain a reliable PSV record. Age models for the studied cores are based on AMS radiocarbon dating of seven and four pollen-enriched samples distributed throughout cores C142a and C087, respectively [*Larrasoaña et al.*, 2011], as no other suitable material for radiocarbon dating was found. The age model of core C142a was developed after correcting some of the samples for a mean reservoir effect of 1182 ± 135 ^{14}C yr BP (see *Larrasoaña et al.* [2011] for a detailed explanation). The same reservoir effect was applied to the four samples from core C087. The constructed age models indicate that the sedimentary records extend back to 1850 yr BC

(core C142a) and 3700 yr BC (core C087), respectively. The resulting mean sedimentation rates (0.39 mm/yr and 0.23 mm/yr for cores C142a and C087, respectively) (Figure 2) are of the same order as sedimentation rates estimated for other cores from Lake Issyk-Kul [*Giralt et al.*, 2004; *Ricketts et al.*, 2001]. An attempt to AMS ^{14}C date the top of core C087 was unsuccessful given the anomalous age of the core top sample. Nevertheless, occurrence of the same uppermost lithological unit in the two studied cores, which have roughly the same thicknesses as those found in previous cores that have been dated using ^{210}Pb [*Giralt et al.*, 2004], suggests that the sediment-water interface was recovered in cores C142a and C087. This is supported by extrapolating linear accumulation rates upward from the uppermost radiocarbon date of each core.

[12] The resulting age models indicate that the sampling resolution in cores C142a and C087 is about 60 and 100 years, respectively. Although this resolution is lower than typical resolutions attained by studying fired archeological materials (where several well-dated structures can be studied per century), it is similar to that of most lake sediment PSV records (mean resolution of about 100 years) used to construct the new generation of global geomagnetic field models [*Donadini et al.*, 2009; *Korte et al.*, 2009].

4. Results

4.1. Rock Magnetism

[13] The low-field magnetic susceptibility of core C142a sediments has roughly constant values of about $0.3*10^{-6}$ m^3/kg down to a depth of ~100 cm, and increases considerably below that depth until reaching a maximum value of $1.2*10^{-6}$ m^3/kg (Figure 3a). Magnetic susceptibility values for core C087 are roughly constant throughout the core, with a mean value of $0.2*10^{-6}$ m^3/kg (Figure 3b) that is similar to the mean susceptibility value for the uppermost 100 cm of core C142a.

[14] S-ratios oscillate around 0.75 throughout most of both cores, which indicate the presence of both low- and high-coercivity magnetic phases. The $IRM_{1.2\ T}/\chi$ ratio has relatively constant values of around 6 and 13 kA/m throughout cores C142a and C087, respectively (Figure 3). These values are consistent with magnetite as the main low-coercivity mineral [*Peters and Dekkers*, 2003] and point to the absence of the (likely authigenic) magnetic iron sulfides greigite or pyrrhotite [e.g., *Larrasoaña et al.*, 2007] despite evidence for the presence of pyrite. The slightly lower $IRM_{1.2\ T}/\chi$ ratios for core C142a suggest coarser magnetite grain sizes compared to core C087 [*Peters and Dekkers*, 2003]. This is further demonstrated by hysteresis data (Figures 4a and 4b), which indicate that cores C087 and C142a are dominated by a low-coercivity mineral that spans the PSD and MD-coarse PSD grain size ranges, respectively. Good correlation between hysteresis parameters and $IRM_{1.2\ T}/\chi$ (Figures 4c and 4d) validates the use of $IRM_{1.2\ T}/\chi$ as a proxy for magnetite grain size throughout the studied cores. Back-field demagnetization data (e.g., Figure 4a, inset) indicate a variable contribution from a high-coercivity mineral, which in the absence of magnetic iron sulfides is interpreted as hematite. The coexistence of this mineral with magnetite is entirely consistent with the S-ratios of the studied sediments [*Frank and Nowaczyk*, 2008].

[15] ARM values of around 20 to $30*10^{-6}$ Am^2/kg are found throughout most of core C087 and parts of core C142a, but ARM values exceed $50*10^{-6}$ Am^2/kg in the lowermost 50 cm of core 142a, in its uppermost 10 cm, and at around 60 cm deep (Figure 3a). HIRM oscillates around ~5 to $\sim 8*10^{-4}$ Am^2/kg in the upper and lower parts of both cores, respectively. Inspection of depth variations of magnetic properties (e.g., χ, ARM, HIRM, $IRM_{1.2\ T}/\chi$) in the studied cores does not reveal a common pattern (Figure 3). Low TOC values (<1.4%) and low Fe contents that undergo minor variations throughout core C142a, with no evidence of sharp shifts (Figure 3a), and preservation of magnetite and hematite indicate relatively little diagenetic modification of the magnetic minerals throughout the studied cores.

4.2. Paleomagnetism

[16] Progressive AF demagnetization of the NRM indicates the presence of a small viscous component in all samples that always unblocks below 15–20 mT (Figure 5). Above this field and up to 80–100 mT, a stable magnetization that is directed toward the origin of the demagnetization plots is identified in all samples except for the two uppermost samples from core C087, which were likely affected by coring disturbances. No evidence for a gyroremanence has been detected in any of the studied samples, which further suggests the lack of magnetic iron sulfides in the studied sediments

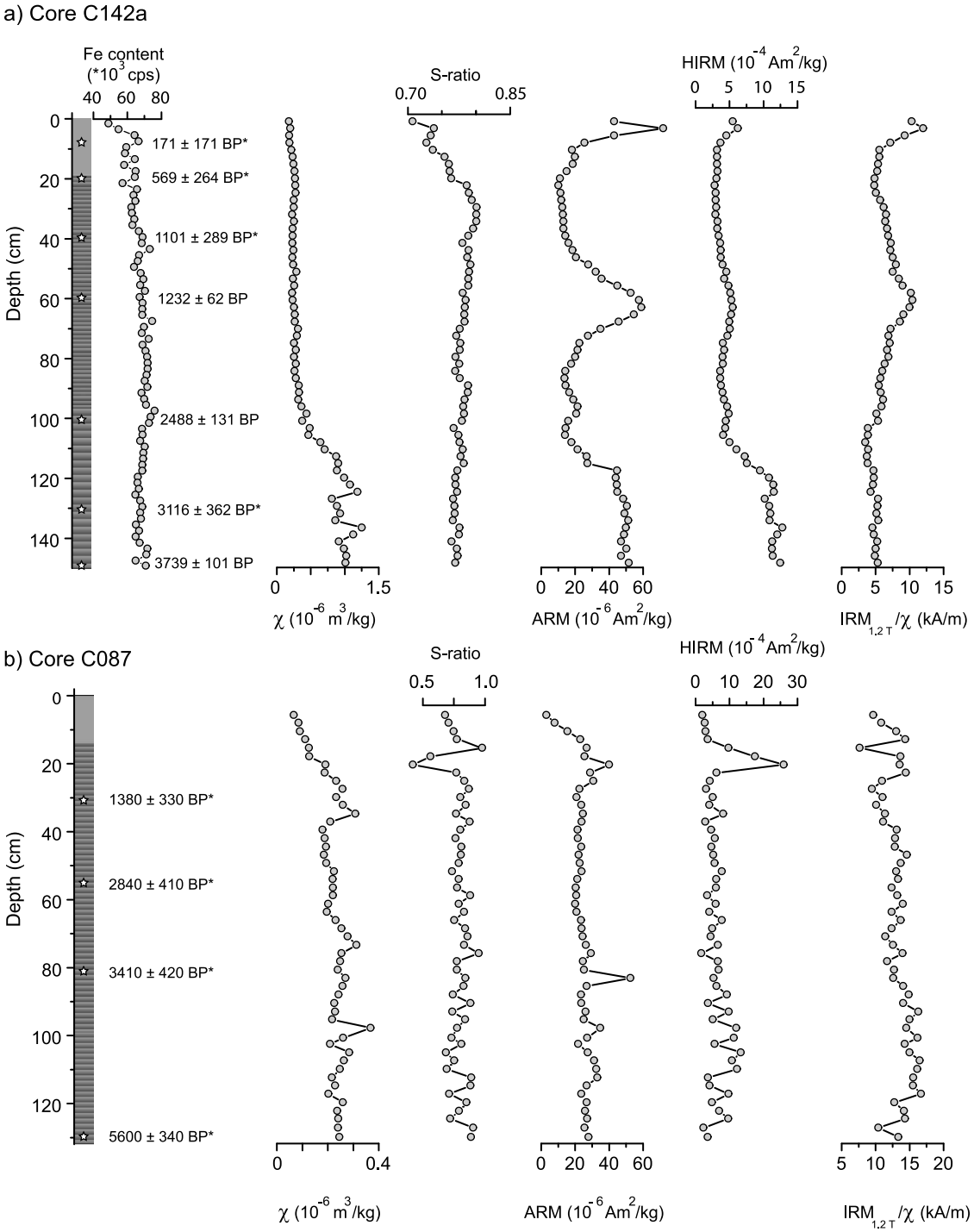

Figure 3. Depth variations of Fe content (Fe, in counts per second from whole-core XRF measurements), low-field magnetic susceptibility (χ), S-ratio, ARM, HIRM, and $IRM_{1.2\ T}/\chi$ for cores (a) C142a and (b) C087. Positions of AMS radiocarbon dates used to construct the age models are indicated (asterisk denotes ages corrected for a reservoir effect; see *Larrasoaña et al.* [2011] for details).

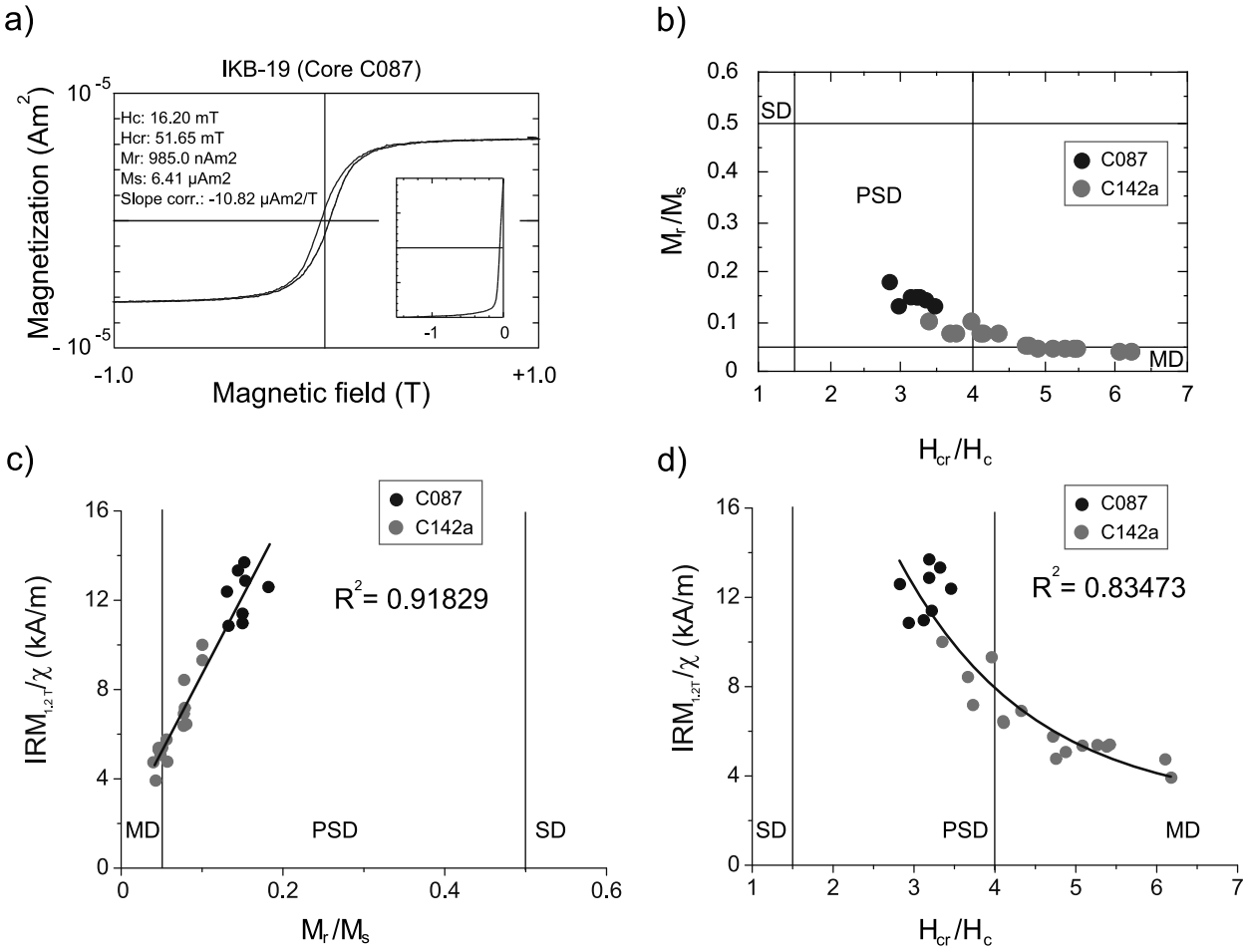

Figure 4. (a) Representative hysteresis loop for the studied Issyk-Kul sediments (after paramagnetic slope correction). Back-field demagnetization data (inset) indicate lack of saturation at 200 mT, and, hence, a contribution from a high-coercivity mineral. (b) Day diagram [*Day et al.*, 1977] for samples from cores C087 and C142a (SD = single domain, PSD = pseudo-single domain, MD = multidomain data fields). (c, d) Correlations among hysteresis parameters (M_r/M_s and H_{cr}/H_c) and $IRM_{1.2\ T}/\chi$.

[e.g., *Snowball*, 1997; *Sagnotti and Winkler*, 1999; *Roberts et al.*, 2011]. The stable remanence component has been interpreted as the characteristic remanent magnetization (ChRM). The maximum angular deviation (MAD) [*Kirschvink*, 1980] obtained for the ChRM directions is generally <5°, with mean MAD values of 4.4° and 2.4° for cores C142a and C087, respectively (Table 1). These low MADs attest to the quality of the calculated ChRM directions [e.g., *Stoner and St-Onge*, 2007], especially for core C087. Mean median destructive fields (MDFs) for cores C142a and C087 are 21 mT and 35.5 mT, respectively. MDF values correlate with $IRM_{1.2\ T}/\chi$, so that lower MDFs correspond to lower $IRM_{1.2\ T}/\chi$ values and, hence, to coarser magnetic grains (Figure 6).

[17] Relevant paleomagnetic and rock-magnetic data are plotted as a function of age after transforming the respective depth scales into age using the independent radiocarbon-based age models for each core (Figure 2) [*Larrasoaña et al.*, 2011]. The mean inclination for core C142a is 34.6° (Figure 6a); inclinations range between 79.3° (1946 AD) and 10.7° (350 BC). Progressively decreasing inclination is observed in this core from 1800 AD to 800 BC. Before this age, inclinations increase sharply and are relatively constant (~35°). The inclination pattern from core C087 (Figure 6b) has important differences in the amplitude of the features observed. For core C087, inclination varies from 61.6° (460 AD) to 33.2° (3560 BC) around a mean of 50.1°.

[18] Cores C142a and C087 are azimuthally unoriented and thus no absolute declination values could be obtained. We plot relative declinations centered around the mean declination for each core

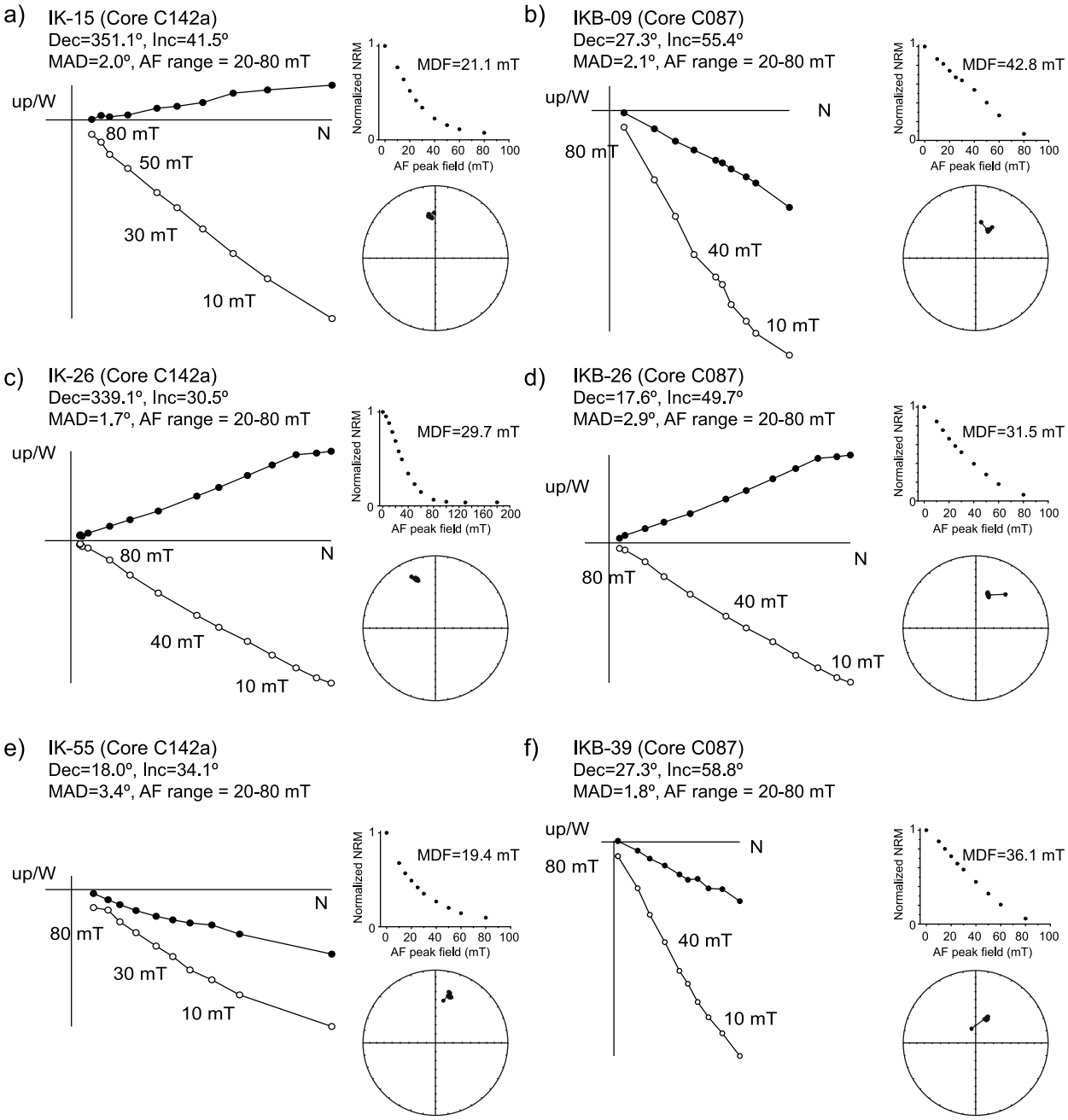

Figure 5. AF demagnetization behavior for representative samples from cores C142a and C087. In the *Zijderveld* [1967] diagrams, open and closed circles represent projections onto the vertical and horizontal planes, respectively. Corresponding stereographic projections and normalized NRM-intensity decay curves are also shown. Numbers indicate the peak applied AF and MDF determined for each sample.

(Figure 6). Relative declinations for core C142a range between −24.1° (at 1721 AD) and 36.1° (1758 BC) and have a relatively flat trend between 1377 AD and 275 BC with a mean value of about −9.5° (Figure 6). Before this age, a progressive increase in declination is observed with a maximum at around 1758 BC. For core C087, relative declinations range between −21.4° (1579 AD) and 17.4° (459 AD). The maximum declination reached at 459 AD is followed by a progressive decrease down to −10.3° at 970 BC. Before this age,

Table 1. Declination and Inclination Data for Cores C142a and C087 From Lake Issyk-Kul[a]

Sample	Depth (cm)	Age (yr AD/BC)	Dec. (deg)	Inc. (deg)	MAD (deg)
		Core C142a (42°34'31.2", 77°20'03.0"E)			
IK01	1.1	1973.0	338.9	55.0	5.1
IK02	3.4	1916.5	348.6	79.3	2.8
IK03	5.8	1857.6	354.6	74.6	2.4
IK04	8.2	1798.6	348.4	78.5	5.8
IK05	10.6	1721.1	327.5	53.7	12.5
IK06	13.0	1634.3	5.8	54.1	9.2
IK07	15.4	1547.4	4.4	64.4	7.3
IK08	17.8	1460.6	357.7	44.6	3.7
IK09	20.2	1377.0	353.3	36.7	6.9
IK10	22.5	1314.5	348.8	27.6	9.2
IK11	25.0	1249.3	351.2	31.9	4.9
IK12	27.4	1184.2	345.9	28.6	8.0
IK13	29.8	1121.7	344.8	36.4	3.5
IK14	32.2	1057.8	344.9	42.1	4.8
IK15	34.6	994.0	351.1	41.5	2.0
IK16	37.0	930.1	350.3	47.5	4.5
IK17	39.4	866.3	350.6	41.0	1.9
IK18	41.7	837.9	346.7	37.0	1.6
IK19	44.1	822.1	347.0	32.0	3.1
IK20	46.5	806.4	348.0	37.7	1.5
IK21	48.9	790.7	342.6	33.8	1.5
IK22	51.3	775.0	343.1	40.8	1.8
IK23	53.7	759.6	340.6	32.9	1.3
IK24	56.0	744.2	341.0	36.6	1.0
IK25	58.4	728.5	341.8	35.2	1.1
IK26	60.8	692.9	339.1	30.5	1.7
IK27	63.2	617.5	341.0	33.9	1.7
IK28	65.6	542.2	341.0	33.4	2.3
IK29	68.0	466.8	336.2	25.2	1.6
IK30	70.4	393.0	336.5	23.9	1.6
IK31	72.7	319.2	338.8	24.9	2.0
IK32	75.1	243.9	337.7	18.7	2.2
IK33	77.5	170.1	337.0	22.4	1.6
IK34	79.8	97.9	336.5	26.2	2.2
IK35	82.1	24.1	337.6	27.4	1.8
IK36	84.5	−51.3	338.2	29.1	2.1
IK37	86.9	−126.7	328.9	24.9	3.7
IK38	89.3	−200.5	334.7	26.0	4.9
IK39	91.6	−274.2	329.8	15.0	4.4
IK40	94.0	−349.6	332.9	10.7	3.3
IK41	96.4	−423.4	336.1	13.3	2.7
IK42	98.7	−497.2	340.5	16.7	2.9
IK43	101.2	−562.1	342.7	18.1	2.8
IK44	103.6	−612.3	349.9	25.1	5.8
IK45	105.9	−660.5	346.9	16.6	6.6
IK46	108.2	−709.7	353.1	11.0	5.0
IK47	110.6	−759.9	5.8	18.4	8.4
IK48	113.0	−809.1	348.3	39.3	6.9
IK49	115.3	−858.3	351.2	37.0	9.3
IK50	117.7	−908.5	3.1	34.1	5.4
IK51	120.1	−957.7	16.8	35.2	5.1
IK52	122.4	−1006.9	10.0	34.6	6.2
IK53	124.8	−1057.1	13.2	30.2	7.7
IK54	127.2	−1106.3	14.2	32.9	6.0
IK55	129.6	−1156.6	18.0	34.1	3.4
IK56	132.0	−1239.3	13.2	34.1	2.8
IK57	134.4	−1325.4	21.2	32.9	2.5
IK58	136.7	−1411.5	17.0	44.9	6.4
IK59	139.1	−1497.7	26.1	34.3	6.3
IK60	141.4	−1583.8	17.4	41.6	4.8

Table 1. (continued)

Sample	Depth (cm)	Age (yr AD/BC)	Dec. (deg)	Inc. (deg)	MAD (deg)
IK61	143.8	−1671.7	18.5	30.6	7.4
IK62	146.2	−1757.9	27.7	33.0	11.6
IK63	148.5	−1849.5	18.0	34.7	5.7
		Core C087 (42°34'5.22", 77°20'10.44"E)			
IKB03	5.9	1683.0	22.26	57.8	2.3
IKB04	8.2	1579.0	5.80	58.0	3.4
IKB05	10.7	1465.9	25.45	53.2	2.4
IKB06	13.1	1357.3	37.29	54.8	1.6
IKB07	15.6	1244.2	32.45	54.1	1.4
IKB08	18.1	1131.0	15.48	56.3	2.0
IKB09	20.5	1022.5	27.28	55.4	2.1
IKB10	22.9	913.9	33.72	61.2	2.0
IKB11	25.3	805.3	38.21	57.9	1.4
IKB12	27.7	696.7	38.66	55.8	1.9
IKB13	30.1	588.1	38.53	57.1	1.4
IKB14	32.4	459.0	44.59	61.6	2.7
IKB15	35.0	307.2	37.34	50.3	2.8
IKB16	37.3	172.9	32.35	49.2	2.9
IKB17	39.7	32.7	37.84	47.4	3.2
IKB18	42.2	−113.3	42.06	48.7	3.4
IKB19	44.7	−259.3	43.29	48.7	2.5
IKB20	47.1	−399.4	39.38	45.4	2.7
IKB21	49.5	−539.6	34.05	42.2	2.9
IKB22	51.9	−679.8	34.70	40.1	1.8
IKB23	54.2	−814.1	30.91	39.6	2.5
IKB24	56.7	−917.4	22.92	37.5	3.2
IKB25	59.0	−969.8	16.93	43.7	3.7
IKB26	61.5	−1026.8	17.57	49.7	2.9
IKB27	63.9	−1081.5	21.08	50.3	1.6
IKB28	66.3	−1136.2	15.58	45.3	4.3
IKB29	68.7	−1191.0	18.82	49.5	1.8
IKB30	71.1	−1245.7	21.06	52.2	2.1
IKB31	73.6	−1302.7	21.80	51.6	3.4
IKB32	76.0	−1357.4	15.29	51.8	0.8
IKB33	78.4	−1412.1	22.44	56.0	2.2
IKB34	80.9	−1477.9	19.38	57.6	3.2
IKB35	83.3	−1585.1	17.77	53.9	1.8
IKB36	85.7	−1692.4	26.73	56.1	1.2
IKB37	88.2	−1804.1	18.40	58.9	2.8
IKB38	90.7	−1915.9	21.55	53.0	2.2
IKB39	93.2	−2027.6	27.29	58.8	1.8
IKB40	95.5	−2130.4	22.97	53.3	1.5
IKB41	98.0	−2242.1	22.98	46.4	2.0
IKB42	100.9	−2371.8	30.24	54.5	3.6
IKB43	102.7	−2452.2	26.51	48.0	1.4
IKB44	105.2	−2563.9	26.74	48.1	1.5
IKB45	107.6	−2671.2	23.48	49.5	3.1
IKB46	110.1	−2782.9	26.16	49.8	1.4
IKB47	112.6	−2894.7	32.79	47.9	2.5
IKB48	115.0	−3001.9	25.30	43.1	2.0
IKB49	117.4	−3109.2	34.06	44.5	2.8
IKB50	119.9	−3220.9	22.53	45.3	3.4
IKB51	122.4	−3332.7	30.17	43.2	2.4
IKB52	124.7	−3435.5	29.65	38.6	2.4
IKB53	127.4	−3556.1	26.04	33.2	4.3
IKB54	130.1	−3676.8	18.63	38.3	3.0

[a]Depths and the corresponding age obtained from the radiocarbon-based age models available for these cores (see *Larrasoaña et al.* [2011] for further details) are indicated for each sample. The maximum angular deviation (MAD) [*Kirschvink*, 1980] obtained for the characteristic remanent magnetizations are also given. The cores were azimuthally unoriented and no absolute declinations could be obtained. Note that only data from core C087 are interpreted as reliable recorders of geomagnetic field changes in the studied area.

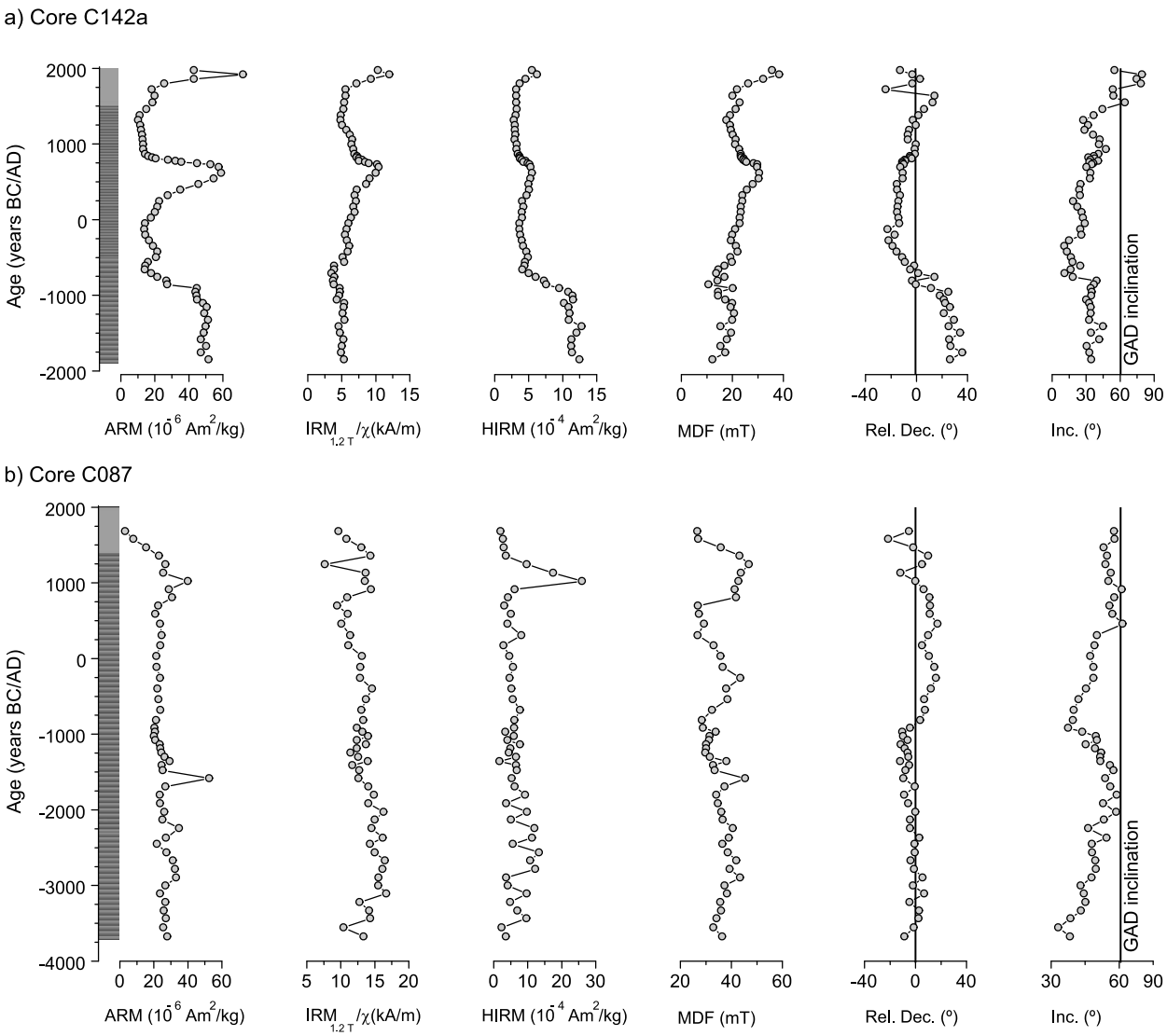

Figure 6. Temporal variations of ARM, $IRM_{1.2\ T}/\chi$, HIRM, median destructive field (MDF) and relative declination and absolute inclination of the characteristic remanent magnetization (ChRM) directions obtained for cores (a) C142a and (b) C087. The inclination expected for a geocentric axial dipole (GAD) field at the site latitude is indicated by a black line. Each record is plotted using its own radiocarbon-based chronology [*Larrasoaña et al.*, 2011].

relatively constant declinations of around −3.5° are observed.

5. Discussion

5.1. PSV Data and Geomagnetic Field Models for Central Asia

[19] Declination and inclination values for cores C087 and C142a are generally consistent between consecutive samples and reveal gradually varying directional changes (Figure 6). These changes appear to be unrelated to variations in lithology or rock magnetic properties, except for the uppermost part of core C142a (Figures 3 and 6). The mean paleomagnetic inclination for core C087 (50.1°) is 11.0° shallower than the expected inclination at the studied site (61.0°) for a geocentric axial dipole (GAD) field (Figure 6). This observed inclination flattening is typical of sediments where the ChRM is a detrital remanent magnetization (DRM) [e.g., *Bressler and Elston*, 1980; *Tauxe*, 2005; *Tauxe et al.*, 2008], and is usually explained as a result of rolling of magnetic particles on the substrate during deposition and further compaction-induced inclination flattening that occurs after locking of the ChRM [*Blow and Hamilton*, 1978; *Anson and Kodama*, 1987; *Tauxe et al.*, 2008]. In contrast,

core C142a has a strikingly stronger average inclination flattening of 26.4°. Amplitudes of declination and inclination variations are about 30° for core C087, which is compatible with expected values at the studied latitude as derived from available data and geomagnetic field models [*Korte and Constable*, 2005; *Korte et al.*, 2005, 2009, and references therein]. In contrast, core C142a has amplitudes of declination and inclination changes of about 60° and 70°, respectively, which are much larger than expected for the studied location. Overall, these circumstances suggest that core C087, but not core C142a, could represent a reliable record of geomagnetic field variations in central Asia. Two main factors may account (perhaps in combination) for the inferred lower paleomagnetic reliability of core C142a. First, the magnetic carriers in these sediments fall mostly within the MD and coarse PSD grain size range (Figure 4). They are therefore less prone to be reliable recorders of stable paleomagnetic directions compared to core C087, which is characterized by finer PSD grain sizes (Figure 4). Second, the magnetic fabric of sediments from core C142a has a stronger tectonic imprint compared to core C087 sediments, probably because of their closer location to an active compressive, E-W oriented fault [*Larrasoaña et al.*, 2011]. Such a tectonic overprint might have altered the spatial configuration of detrital magnetic particles in core C142a, thereby affecting the ChRM directions. Factors such as differential compaction after locking of the ChRM might also have affected the paleomagnetic recording fidelity of core C142a. Regardless of the specific cause(s), we consider that core C142 does not provide a reliable record of PSV at the studied site, so that only results from core C087 are hereafter considered.

[20] PSV data from core C087 from Lake Issyk-Kul are shown in Figure 7 along with PSV records from Lake Baikal, Lake Aslikul and the Aral Sea. A strikingly similar pattern can be observed between the inclination records from lakes Issyk-Kul and Baikal (Figure 7). Relative inclination minima at around 750–1000 BC and 3500 BC, along with inclination maxima at around 750 AD and 2000 BC, are observed for both records. The declination records from lakes Issyk-Kul and Baikal have some similarities such as the occurrence of relative declination maxima at around 1250 AD, 250 BC, and 3250 BC, but also some significant discrepancies in the ages of declination minima (Figure 7). Given the large distance between lakes Issyk-Kul and Baikal (about 2300 km) and their independent radiocarbon chronologies, we consider their records to be remarkably consistent. The inclination record from Lake Aslikul has a similar structure to those of lakes Issyk-Kul and Baikal, although some features appear to be shifted to younger ages before 500 AD (Figure 7). This is the case for the inclination maximum at around 1250 BC and the minima at 250 BC and 2500 BC in Lake Aslikul, which occur at 2000 BC, 750–1000 BC, and 3500 BC, respectively, in lakes Issyk-Kul and Baikal. A similar shift to younger ages seems to occur in the main features of the Aslikul declination record compared to lakes Issyk-Kul and Baikal (Figure 7), although such shifts are less clear because of the less marked similarities among the records. Overall, this suggests a 500–1000 year offset to younger ages inferred before 500 AD for Lake Aslikul on the basis of inclination data. The Aral Sea record is too short to enable reliable comparison.

[21] The family of spherical harmonic geomagnetic models [*Korte and Constable*, 2005; *Korte et al.*, 2009], which includes the SED3K.1 (based only on lacustrine and rapidly accumulated marine sediments), ARCH3K.1 (based only on archeological and lava flow material) and CALS7K.2 models (based on all sources of paleomagnetic data), appear to reproduce, albeit with some differences in amplitude and resolution, the PSV recorded in Lake Aslikul (Figure 7). In contrast, the models reproduce well the structure of the PSV records from lakes Issyk-Kul and Baikal, although there appears to be a significant temporal offset before 500 AD. The records appear to be shifted to older ages, with offsets ranging between 500 and 1000 years.

[22] There are three alternative explanations for the observed age offsets among the PSV records. The first is that the features identified in the lakes Issyk-Kul and Baikal records constitute genuine non-dipolar features that are captured later in the west in Lake Aslikul. This interpretation is ad hoc and is difficult to support on geomagnetic grounds. Age differences of 500–1000 years are too large to be explained solely by westward drift of higher-term geomagnetic field components [*Snowball et al.*, 2007]. The second possibility is that the lakes Issyk-Kul and Baikal PSV records are based on problematic chronologies linked, for example, to an undetected and/or time variable reservoir effect that yields older radiocarbon ages for sediments older than 500 AD. Given the distance and the striking differences in size and water chemistry between lakes Issyk-Kul and Baikal, [*Herdendorf*, 1982; *Savvaitova and Petr*, 1992], and keeping in mind the similarity between their PSV records, we

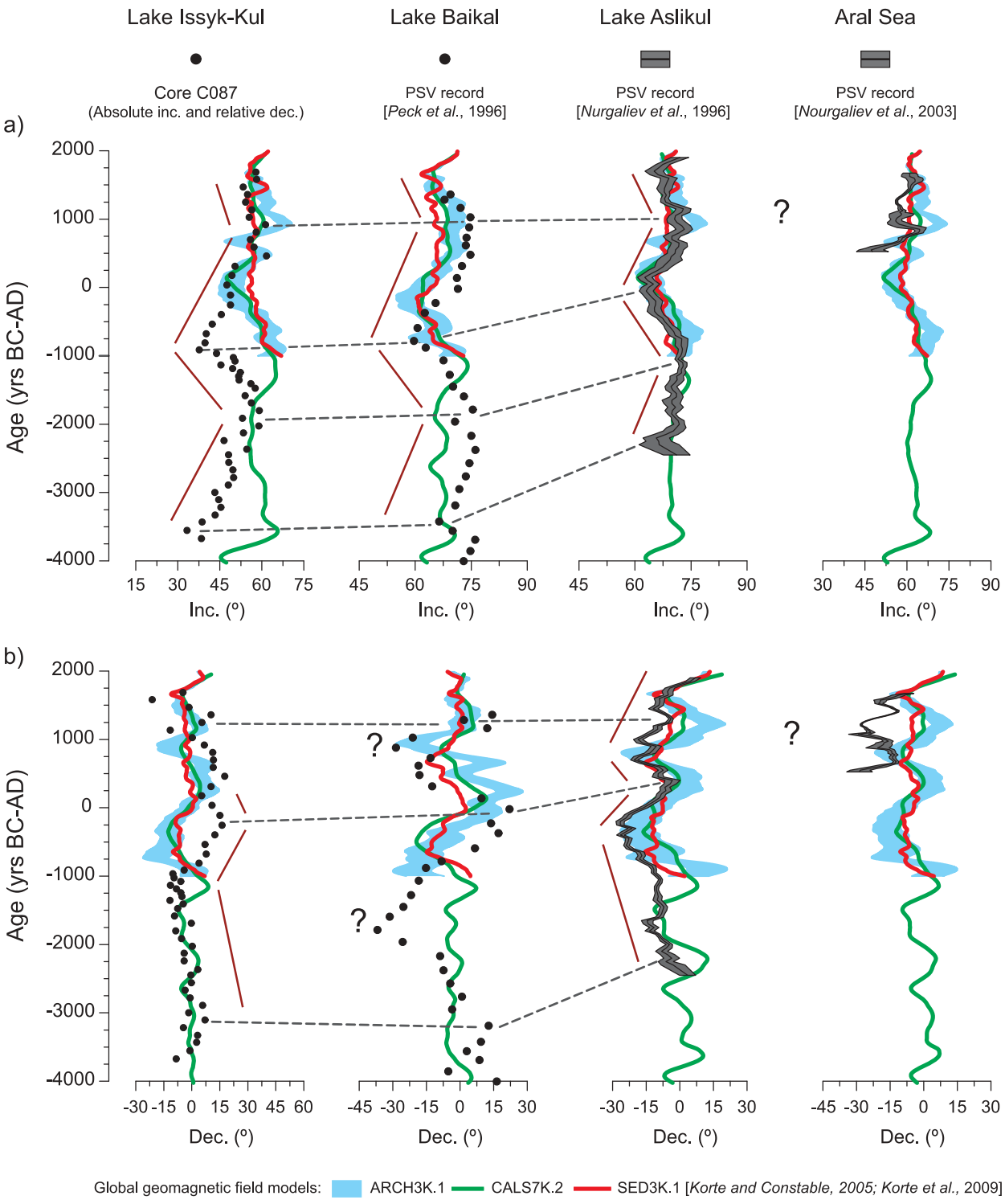

Figure 7. Comparison between the new PSV record obtained for Lake Issyk-Kul and published data from Lake Baikal [*Peck et al.*, 1996], Lake Aslikul [*Nurgaliev et al.*, 1996] and Aral Sea [*Nourgaliev et al.*, 2003]. Declination and inclination values predicted for each location from geomagnetic field models [*Korte and Constable*, 2005; *Korte et al.*, 2009] are also shown. Distinctive inclination and declination features are correlated and are labeled with dashed lines.

consider this explanation unlikely. The third possibility is that the Lake Aslikul PSV record is shifted to younger ages due to either a delayed remanence acquisition [e.g., *Sagnotti et al.*, 2005; *Suganuma et al.*, 2011] or to an inaccurate chronological model. The age model for the Lake Aslikul record is not based on radiocarbon dating but on a correlation between a pollen-based paleoclimatic record and a radiocarbon-dated regional paleotemperature master curve [*Klimanov and Khotinsky*, 1988, pp. 45–51; *Nurgaliev et al.*, 1996]. Keeping in mind the lack of a direct chronology for this record, we consider this explanation to be the most plausible. In this case, the discrepancies between the lakes Issyk-Kul and Baikal PSV records and the SED3K.1 and CALS7K.2 models might be explained by a strong temporal bias on the model results exerted by the Lake Aslikul record. However, this interpretation is difficult to reconcile with the ARCH3K.1 model (Figure 7), which has similar PSV trends to those of models SED3K.1 and CALS7K.2 and is independent of sedimentary PSV data. It should be noted, however, that the number of archeologic- and lava flow-derived PSV data decreases significantly for the first millennia BC in central Asia [*Donadini et al.*, 2009], so there is the potential that future improvements in the number of source data for this period will improve the ARCH3K.1 model in the Lake Issyk-Kul region.

5.2. Environmental Implications

[23] The terrigenous fraction of the Holocene Lake Issyk-Kul sediments derives from the combined supply of riverine suspended material from the Jergueland and Tyup rivers and eolian dust sourced from the Taklamakan Desert [*De Batist et al.*, 2002; *Giralt et al.*, 2004]. Magnetite is ubiquitous in metamorphic, intrusive and volcanic rocks [*Dunlop and Özdemir*, 1997], such as those that dominate the catchment of Lake Issyk-Kul, and is also the main magnetic mineral in surface samples from the Taklamakan Desert [*Torii et al.*, 2001]. Eolian dust from the Taklamakan Desert has been shown to contain hematite [*Torii et al.*, 2001], which might also be common in the metamorphic, intrusive and volcanic rocks [*Dunlop and Özdemir*, 1997] of the Lake Issyk-Kul catchment. Hematite is therefore the most likely high-coercivity mineral in the studied sediments from Lake Issyk-Kul. Temporal variations in magnetite and hematite concentrations (as identified by variations in ARM and HIRM, respectively) in the two studied cores do not have a common pattern (Figure 6). The presence of both minerals in all potential terrigenous source sediments prevents reliable interpretation of magnetite and hematite abundances in terms of paleoenvironmental (riverine and dust) variations in the Lake Issyk-Kul area. Hysteresis and $IRM_{1.2\ T}/\chi$ data indicate the presence of coarser-grained magnetite in core C142a sediments, which is consistent with sedimentological evidence for a higher sand content in this core and its location within a distributary channel of the deltaic system that drains into Lake Issyk-Kul from the NNW (Figure 1d). $IRM_{1.2\ T}/\chi$ data do not have common variations in the two studied cores (Figure 6). More detailed rock magnetic studies are necessary to disentangle the environmental significance of magnetic mineralogic variations in the studied records.

6. Conclusions

[24] Stable paleomagnetic results from core C087 and an independent radiocarbon-based chronology indicate that mid to late Holocene sediments recovered from Lake Issyk-Kul provide a reliable record of PSV changes in central Asia. This is further supported by the overall similarity found between PSV records from lakes Issyk-Kul and Baikal, which are the only available Holocene central Asian PSV records with independent radiocarbon-based chronologies. Although similar in structure, significant temporal offsets before 500 AD exist between these two PSV records and those of Lake Aslikul and from global geomagnetic field models. We attribute the age offsets to the indirect age model on which the Lake Aslikul PSV record is based and to the strong bias that this record exerts on the global model results. Although additional well-dated PSV records are still needed to obtain a more robust understanding of regional PSV in central Asia and to improve geomagnetic field models, our new data represent a step in this direction. Our results also illustrate the potential of PSV records as a tool for dating sedimentary sequences, especially by matching inclination features, in a region that is key for unraveling teleconnections between high- and low-latitude climatic processes [*Rohling et al.*, 2009; *Yang et al.*, 2009]. Available bulk rock magnetic data have proved unsuccessful for disentangling past environmental changes in the Lake Issyk-Kul region, likely because magnetite and hematite, the two main magnetic minerals in the studied sediments, have a mixed (fluvial and eolian) terrigenous origin.

Acknowledgments

[25] Financial support for this research was provided through a CSIC JAE-Doc post-doctoral research contract (MGP), the GRACCIE (Spanish Consolider-Ingenio CSD2007-00067), APELIK (EU ICA2-CT-2000-10003), CGL2008-02203/BTE, and PALEONAO (CGL2010-15767/BTE) research projects. We thank D. Nourgaliev for providing additional information concerning the Lake Aslikul and Aral Sea paleomagnetic records and four anonymous referees and the Associate Editor for their valuable, thorough and constructive comments that greatly improved this paper.

References

Ali, M., H. Oda, A. Hayashida, K. Takemura, and M. Torii (1999), Holocene palaeomagnetic secular variation at Lake Biwa, central Japan, *Geophys. J. Int.*, *136*, 218–228, doi:10.1046/j.1365-246X.1999.00718.x.

Anson, G. L., and K. P. Kodama (1987), Compaction-induced inclination shallowing of the post-depositional remanent magnetization in a synthetic sediment, *Geophys. J. R. Astron. Soc.*, *88*, 673–692, doi:10.1111/j.1365-246X.1987.tb01651.x.

Bard, E., and G. Delaygue (2008), Comment on "Are there connections between the Earth's magnetic field and climate?" by V. Courtillot et al., *Earth Planet. Sci. Lett.*, *265*, 302–307, doi:10.1016/j.epsl.2007.09.046.

Barletta, F., G. St-Onge, J. E. T. Channell, and A. Rochon (2010), Dating of Holocene western Canadian Arctic sediments by matching paleomagnetic secular variation to a geomagnetic field model, *Quat. Sci. Rev.*, *29*, 2315–2324, doi:10.1016/j.quascirev.2010.05.035.

Bloemendal, J., J. W. King, F. R. Hall, and S. J. Doh (1992), Rock magnetism of late Neogene and Pleistocene deep-sea sediments: Relationship to sediment source, diagenetic processes, and sediment lithology, *J. Geophys. Res.*, *97*, 4361–4375, doi:10.1029/91JB03068.

Blow, R. A., and N. Hamilton (1978), Effect of compaction on acquisition of a detrital remanent magnetization in fine-grained sediments, *Geophys. J. R. Astron. Soc.*, *52*, 13–23, doi:10.1111/j.1365-246X.1978.tb04219.x.

Bressler, S. L., and D. P. Elston (1980), Declination and inclination errors in experimentally deposited specularite-bearing sand, *Earth Planet. Sci. Lett.*, *48*, 227–232, doi:10.1016/0012-821X(80)90184-3.

Courtillot, V., Y. Gallet, J. L. Le Mouël, F. Fluteau, and A. Genevey (2007), Are there connections between the Earth's magnetic field and climate?, *Earth Planet. Sci. Lett.*, *253*, 328–339, doi:10.1016/j.epsl.2006.10.032.

Day, R., M. Fuller, and V. A. Schmidt (1977), Hysteresis properties of titanomagnetites: Grain size and composition dependence, *Phys. Earth Planet. Inter.*, *13*, 260–267, doi:10.1016/0031-9201(77)90108-X.

De Batist, M., J. Klerkx, Y. Imbo, S. Giralt, V. Lignier, C. Beck, D. Delvaux, P. Vermeesch, I. Kalugin, and K. Abdrachmatov (2002), Bathymetry and sedimentary environments of a large, high-altitude, tectonic lake: Lake Issyk-Kul, Kyrgyz Republic (central Asia), in *The Issyk-Kul Lake: Evaluation of Environmental State and Its Remediation*, *NATO ASI Ser., IV*, vol. 13, edited by J. Klerkx and B. Imanackunov, pp. 101–124, Kluwer Acad., Dordrecht, Netherlands, doi:10.1007/978-94-010-0491-6_9.

Donadini, F., M. Korte, and C. G. Constable (2009), Geomagnetic field for 0–3 ka: New data sets for global modeling, *Geochem. Geophys. Geosyst.*, *10*, Q06007, doi:10.1029/2008GC002295.

Dunlop, D. J. (2002), Theory and application of the Day plot (M_{rs}/M_s versus H_{cr}/H_c): 2. Application to data for rocks, sediments and soils, *J. Geophys. Res.*, *107*(B3), 2057, doi:10.1029/2001JB000487.

Dunlop, D. J., and Ö. Özdemir (1997), *Rock Magnetism, Fundamentals and Frontiers*, Cambridge Univ. Press, Cambridge, U. K., doi:10.1017/CBO9780511612794.

Evans, M. E., and F. Heller (2003), *Environmental Magnetism*, Academic, San Diego, Calif.

Frank, U., and N. R. Nowaczyk (2008), Mineral magnetic properties of artificial samples systematically mixed from haematite and magnetite, *Geophys. J. Int.*, *175*, 449–461, doi:10.1111/j.1365-246X.2008.03821.x.

Frank, U., N. R. Nowaczyk, J. F. W. Negendank, and M. Melles (2002), A paleomagnetic record from Lake Lama, northern Central Siberia, *Phys. Earth Planet. Inter.*, *133*, 3–20, doi:10.1016/S0031-9201(02)00088-2.

Gallet, Y., A. Genevey, and F. Fluteau (2005), Does Earth's magnetic field secular variation control centennial climate change?, *Earth Planet. Sci. Lett.*, *236*, 339–347, doi:10.1016/j.epsl.2005.04.045.

Giralt, S., S. Riera, J. Klerkx, R. Julià, V. Lignier, C. Beck, M. De Batist, and I. Kalugin (2002), Recent paleoenvironmental evolution of Lake Issyk-Kul, in *The Issyk-Kul Lake: Evaluation of Environmental State and Its Remediation*, *NATO ASI Ser., IV*, vol. 13, edited by J. Klerkx and B. Imanackunov, pp. 125–145, Kluwer Acad., Dordrecht, Netherlands, doi:10.1007/978-94-010-0491-6_10.

Giralt, S., et al. (2004), 1000 year environmental history of Lake Issyk-Kul, in *Dying and Dead Seas: Climatic Versus Anthropic Causes*, *NATO ASI Ser., IV*, vol. 36, edited by J. C. J. Nihoul, P. O. Zavialov, and P. P. Micklin, pp. 253–285, Kluwer Acad., Dordrecht, Netherlands, doi:10.1007/978-94-007-0967-6_10.

Gómez-Paccard, M., A. Chauvin, P. Lanos, G. McIntosh, M. L. Osete, G. Catanzariti, V. C. Ruiz-Martinez, and J. I. Nuñez (2006), First archaeomagnetic secular variation curve for the Iberian Peninsula: Comparison with other data from western Europe and with global geomagnetic field models, *Geochem. Geophys. Geosyst.*, *7*, Q12001, doi:10.1029/2006GC001476.

Gómez-Paccard, M., A. Chauvin, P. Lanos, and J. Thiriot (2008), New archeointensity data from Spain and the geomagnetic dipole moment in western Europe over the past 2000 years, *J. Geophys. Res.*, *113*, B09103, doi:10.1029/2008JB005582.

Herdendorf, C. E. (1982), Large lakes of the world, *J. Great Lakes Res.*, *8*, 379–412, doi:10.1016/S0380-1330(82)71982-3.

Irurzun, M. A., C. G. S. Gogorza, M. A. E. Chaparro, J. M. Lirio, H. Nuñez, J. F. Vilas, and A. M. Sinito (2006), Paleosecular variations recorded by Holocene-Pleistocene sediments from Lake El Trébol (Patagonia, Argentina), *Phys. Earth Planet. Inter.*, *154*, 1–17, doi:10.1016/j.pepi.2005.06.012.

Irurzun, M. A., C. G. S. Gogorza, A. M. Sinito, M. A. E. Chaparro, H. Nuñez, and J. M. Lirio (2008), Paleosecular variations 12–20 kyr as recorded by sediments from Lake Moreno (southern Argentina), *Stud. Geophys. Geod.*, *52*, 157–172, doi:10.1007/s11200-008-0011-5.

Kirschvink, J. L. (1980), The least-squares line and plane and the analysis of paleomagnetic data, *Geophys. J. R. Astron. Soc.*, *62*, 699–718, doi:10.1111/j.1365-246X.1980.tb02601.x.

Klimanov, V. A., and N. A. Khotinsky (Eds.) (1988), *Paleoclimates of the Holocene of the European Part of USSR* [in Russian], Inst. Geogr. Sci. Acad. USSR, Moscow.

Korte, M., and C. G. Constable (2005), Continuous geomagnetic field models for the past 7 millennia: 2. CALS7K, *Geochem. Geophys. Geosyst.*, *6*, Q02H16, doi:10.1029/2004GC000801.

Korte, M., A. Genevey, C. G. Constable, U. Frank, and E. Schnepp (2005), Continuous geomagnetic field models for the past 7 millennia: 1. A new global data compilation, *Geochem. Geophys. Geosyst.*, *6*, Q02H15, doi:10.1029/2004GC000800.

Korte, M., F. Donadini, and C. G. Constable (2009), Geomagnetic field for 0–3 ka: 2. A new series of time-varying global models, *Geochem. Geophys. Geosyst.*, *10*, Q06008, doi:10.1029/2008GC002297.

Kruiver, P. P., and H. F. Passier (2001), Coercivity analysis of magnetic phases in sapropel S1 related to variations in redox conditions, including an investigation of the S ratio, *Geochem. Geophys. Geosyst.*, *2*(12), 1063, doi:10.1029/2001GC000181.

Larrasoaña, J. C., A. P. Roberts, R. J. Musgrave, E. Gracia, E. Pinero, M. Vega, and F. Martinez-Ruiz (2007), Diagenetic formation of greigite and pyrrhotite in gas hydrate marine sedimentary systems, *Earth Planet. Sci. Lett.*, *261*, 350–366, doi:10.1016/j.epsl.2007.06.032.

Larrasoaña, J. C., M. Gómez-Paccard, S. Giralt, and A. P. Roberts (2011), Rapid locking of tectonic magnetic fabrics in weakly deformed mudrocks, *Tectonophysics*, *507*, 16–25, doi:10.1016/j.tecto.2011.05.003.

Lisé-Pronovost, A., G. St-Onge, S. Brachfeld, F. Barletta, and D. Darby (2009), Paleomagnetic constraints on the Holocene stratigraphy of the Arctic Alaskan margin, *Global Planet. Change*, *68*, 85–99, doi:10.1016/j.gloplacha.2009.03.015.

Muscheler, R., J. Beer, P. W. Kubik, and H. A. Synal (2005), Geomagnetic field intensity during the last 60,000 years based on ^{10}Be and ^{36}Cl from the Summit ice cores and ^{14}C, *Quat. Sci. Rev.*, *24*, 1849–1860, doi:10.1016/j.quascirev.2005.01.012.

Néel, L. (1955), Some theoretical aspects of rock-magnetism, *Adv. Phys.*, *4*, 191–243, doi:10.1080/00018735500101204.

Nourgaliev, D. K., F. Heller, A. S. Borisov, I. Hajdas, G. Bonani, P. G. Iassonov, and H. Oberhänsli (2003), Very high resolution paleosecular variation record for the last ~1200 years from the Aral Sea, *Geophys. Res. Lett.*, *30*(17), 1914, doi:10.1029/2003GL018145.

Nurgaliev, D. K., A. S. Borisov, F. Heller, B. V. Burov, P. G. Jasonov, D. I. Khasanov, and S. Z. Ibragimov (1996), Geomagnetic secular variation through the last 3500 years as recorded by Lake Aslikul sediments from eastern Europe (Russia), *Geophys. Res. Lett.*, *23*, 375–378, doi:10.1029/96GL00258.

Pavón-Carrasco, F. J., M. L. Osete, J. M. Torta, and L. R. Gaya-Piqué (2009), A regional archeomagnetic model for Europe for the last 3000 years, SCHA.DIF.3K: Applications to archeomagnetic dating, *Geochem. Geophys. Geosyst.*, *10*, Q03013, doi:10.1029/2008GC002244.

Peck, J. A., J. W. King, S. M. Colman, and V. A. Kravchinsky (1996), An 84-kyr paleomagnetic record from the sediments of Lake Baikal, Siberia, *J. Geophys. Res.*, *101*, 11,365–11,385, doi:10.1029/96JB00328.

Peters, C., and M. J. Dekkers (2003), Selected room temperature magnetic parameters as a function of mineralogy, concentration and grain size, *Phys. Chem. Earth*, *28*, 659–667, doi:10.1016/S1474-7065(03)00120-7.

Ricketts, N. R., T. C. Johnson, E. T. Brown, K. A. Rasmussen, and V. V. Romanovsky (2001), The Holocene paleolimnology of Lake Issyk-Kul, Kyrgyzstan: Trace element and stable isotope composition of ostracodes, *Palaeogeogr. Palaeoclimatol. Palaeoecol.*, *176*, 207–227, doi:10.1016/S0031-0182(01)00339-X.

Roberts, A. P., L. Chang, C. J. Rowan, C.-S. Horng, and F. Florindo (2011), Magnetic properties of sedimentary greigite (Fe_3S_4): An update, *Rev. Geophys.*, *49*, RG1002, doi:10.1029/2010RG000336.

Rohling, E. J., Q. S. Liu, A. P. Roberts, J. D. Stanford, S. O. Rasmussen, P. L. Langen, and M. Siddall (2009), Controls on the East Asian monsoon during the last glacial cycle, based on comparison between Hulu Cave and polar ice-core records, *Quat. Sci. Rev.*, *28*, 3291–3302, doi:10.1016/j.quascirev.2009.09.007.

Sagnotti, L., and A. Winkler (1999), Rock magnetism and palaeomagnetism of greigite-bearing mudstones in the Italian peninsula, *Earth Planet. Sci. Lett.*, *165*, 67–80, doi:10.1016/S0012-821X(98)00248-9.

Sagnotti, L., F. Budillon, J. Dinarès-Turell, M. Iorio, and P. Macri (2005), Evidence for a variable paleomagnetic lock-in depth in the Holocene sequence from the Salerno Gulf (Italy): Implications for "high-resolution" paleomagnetic dating, *Geochem. Geophys. Geosyst.*, *6*, Q11013, doi:10.1029/2005GC001043.

Savvaitova, K., and T. Petr (1992), Lake Issyk-Kul, Kirgizia, *Int. J. Salt Lake Res.*, *1*, 21–46, doi:10.1007/BF02904361.

Snowball, I. F. (1997), The detection of single-domain greigite (Fe_3S_4) using rotational remanent magnetization (RRM) and the effective gyro field (B_g): Mineral magnetic and palaeomagnetic applications, *Geophys. J. Int.*, *130*, 704–716, doi:10.1111/j.1365-246X.1997.tb01865.x.

Snowball, I., and R. Muscheler (2007), Palaeomagnetic intensity data: An Achilles heel of solar activity reconstructions, *Holocene*, *17*, 851–859, doi:10.1177/0959683607080531.

Snowball, I., L. Zillén, A. Ojala, T. Saarinen, and P. Sandgren (2007), FENNOSTACK and FENNORPRIS: Varve dated Holocene palaeomagnetic secular variation and relative palaeointensity stacks for Fennoscandia, *Earth Planet. Sci. Lett.*, *255*, 106–116, doi:10.1016/j.epsl.2006.12.009.

Stockhausen, H. (1998), Geomagnetic palaeosecular variation (0–13,000 yr BP) as recorded in sediments from three maar lakes from the West Eifel (Germany), *Geophys. J. Int.*, *135*, 898–910, doi:10.1046/j.1365-246X.1998.00664.x.

Stoner, J. S., and G. St-Onge (2007), Magnetic stratigraphy in paleoceanography: Reversals, excursions, paleointensity, and secular variation, in *Proxies in Late Cenozoic Paleoceanography*, *Dev. in Mar. Geol.*, vol. 1, edited by C. Hillaire-Marcel and A. deVernal, pp. 99–138, Elsevier, Amsterdam, doi:10.1016/S1572-5480(07)01008-1.

Suganuma, Y., J. Okuno, D. Heslop, A. P. Roberts, T. Yamazaki, and Y. Yokoyama (2011), Post-depositional remanent magnetization lock-in for marine sediments deduced from ^{10}Be and paleomagnetic records through the Matuyama-Brunhes boundary, *Earth Planet. Sci. Lett.*, *311*, 39–52, doi:10.1016/j.epsl.2011.08.038.

Tauxe, L. (2005), Inclination flattening and the geocentric axial dipole hypothesis, *Earth Planet. Sci. Lett.*, *233*, 247–261, doi:10.1016/j.epsl.2005.01.027.

Tauxe, L., K. P. Kodama, and D. V. Kent (2008), Testing corrections for paleomagnetic inclination error in sedimentary rocks: A comparative approach, *Phys. Earth Planet. Inter.*, *169*, 152–165, doi:10.1016/j.pepi.2008.05.006.

Thompson, R., and F. Oldfield (1986), *Environmental Magnetism*, Allen and Unwin, Boston, Mass.

Torii, M., T.-Q. Lee, K. Fukuma, T. Mishima, T. Yamazaki, H. Oda, and N. Ishikawa (2001), Mineral magnetic study of the Taklimakan desert sands and its relevance to the Chinese loess, *Geophys. J. Int.*, *146*, 416–424, doi:10.1046/j.0956-540x.2001.01463.x.

Torizin, J., G. Jentzch, P. Malischewsky, J. Kley, N. Abakanov, and A. Kurskeev (2009), Rating of seismicity and reconstruction of the fault geometries in northern Tien Shan within the project "Seismic Hazard Assessment for Almaty," *J. Geodyn.*, *48*, 269–278, doi:10.1016/j.jog.2009.09.030.

Verosub, K. L., and A. P. Roberts (1995), Environmental magnetism: Past, present and future, *J. Geophys. Res.*, *100*, 2175–2192, doi:10.1029/94JB02713.

Vigliotti, L. (2006), Secular variation record of the Earth's magnetic field in Italy during the Holocene: Constraints for the construction of a master curve, *Geophys. J. Int.*, *165*, 414–429, doi:10.1111/j.1365-246X.2005.02785.x.

Wollin, G., D. B. Ericson, and W. B. F. Ryan (1978), Climatic changes, magnetic intensity variations and fluctuations of eccentricity of Earth's orbit during past 2,000,000 years and mechanism which may be responsible for relationship, *Earth Planet. Sci. Lett.*, *41*, 395–397, doi:10.1016/0012-821X(78)90170-X.

Yang, B., J. Wang, A. Bräuning, Z. B. Dong, and J. Esper (2009), Late Holocene climatic and environmental changes in arid central Asia, *Quat. Int.*, *194*, 68–78., doi:10.1016/j.quaint.2007.11.020

Zabirov, R. D., and V. N. Korotaev (1978), Location and morphometry of the lake [in Russian], in *Lake Issyk-Kul*, pp. 12–20, Illim, Frunze, Tajikistan.

Zijderveld, J. D. A. (1967), Demagnetization of rocks: Analysis of results, in *Methods in Palaeomagnetism*, edited by D. W. Collinson et al., pp. 254–286, Elsevier, Amsterdam.